Computation of Ion Trajectories in the Monopole Mass Spectrometer by Numerical Integration of Mathieu's Equation*

Abstract: A high speed digital computer used with an off-line curve plotter enabled ion trajectories to be readily obtained in terms of the initial conditions and the parameters appearing in the differential equation of motion (Mathieu's equation). A study of these trajectories has led to the conclusion that ions should not be injected parallel to the axis of the instrument, as is done at present, but through the axis and at an angle to it. A simple empirical expression enables the variation of position of ion focus with mass and operating parameters to be predicted.

Introduction

As vacuum techniques have become more sophisticated, increasing attention has been paid to the chemical composition of the gaseous mixtures in high vacuum systems, in addition to the total quantity as measured in an ionization gauge. The ionization gauge operates by bombarding the gas with electrons of about 100 eV energy, collecting the resulting ions at a collector electrode, and measuring the ion current with an electrometer. The ion currents involved can be extremely small; for example, a pressure of 10^{-12} atmospheres typically yields an ion current of 10^{-10} ampere. Nevertheless, the chemical composition of the gas can be determined by separating ions of different charge/mass ratio and measuring separately the currents that are due to the different ion species. For chemical analysis in high and ultra-high vacuum systems, such a mass analyzer must be of simple and rugged construction, must be bakeable, and must have sufficient resolving power to completely separate adjacent masses. The high resolution that is needed to detect mass defects is not needed in chemical analysis.

The mass analyzer that has been most widely used is the familiar magnetic analyzer, in which a monoenergetic beam of ions is injected into a uniform magnetic field at right angles to the direction of ion motion; the ions then take on circular trajectories whose curvature is proportional to the square root of the charge/mass ratio. After the pioneering work of Paul et al., however, there has been strong interest in radiofrequency analyzers of the quadrupole type. These instruments have advantages in that they do not require a magnet and are equally

convenient for high or low masses; further, the quadrupole does not require a well-defined ion injection velocity. Although the monopole mass spectrometer has a similar field configuration, it requires that the ion injection be well-defined. At the same time it has the important merit that its resolving power is less limited by the velocity spread in the ion beam than is that of a magnetic analyzer.

A further distinction between the magnetic analyzer and the monopole instrument is that the circular ion trajectories of the former are well known and easily calculated, while those of the latter are highly complex, difficult to treat analytically and, except for one example given by von Zahn, not available in graphic form. The purpose of this paper is to offer an extensive compilation of trajectories derived for the monopole instrument through computer solutions to the differential equations that obtain.

In both the monopole and quadrupole mass spectrometers, 1,2 ions are caused to oscillate in the segment of the electric quadrupole field described by

$$\phi = [(x^2 - y^2)/r_0^2](U + V \cos \omega t), \tag{1}$$

for which y > |x|. This field has equipotentials in the form of rectangular hyperbolae with asymptotes $y = \pm x$. It has the desirable property, xy terms being absent, that $(\partial \phi/\partial x)$ and $(\partial \phi/\partial y)$, the x and y components of the electric field, are independent of y and x respectively, so that the motion of the ions may be resolved into independent x and y vibrations. Since $(\partial \phi/\partial z) = 0$, the z component of the motion is a steady drift determined by

^{*} Sponsored in part by the Air Force Office of Scientific Research of the Office of Aerospace Research under Contract AF 49(638)-1201.

[†] A summary of nomenclature is given on page 39.

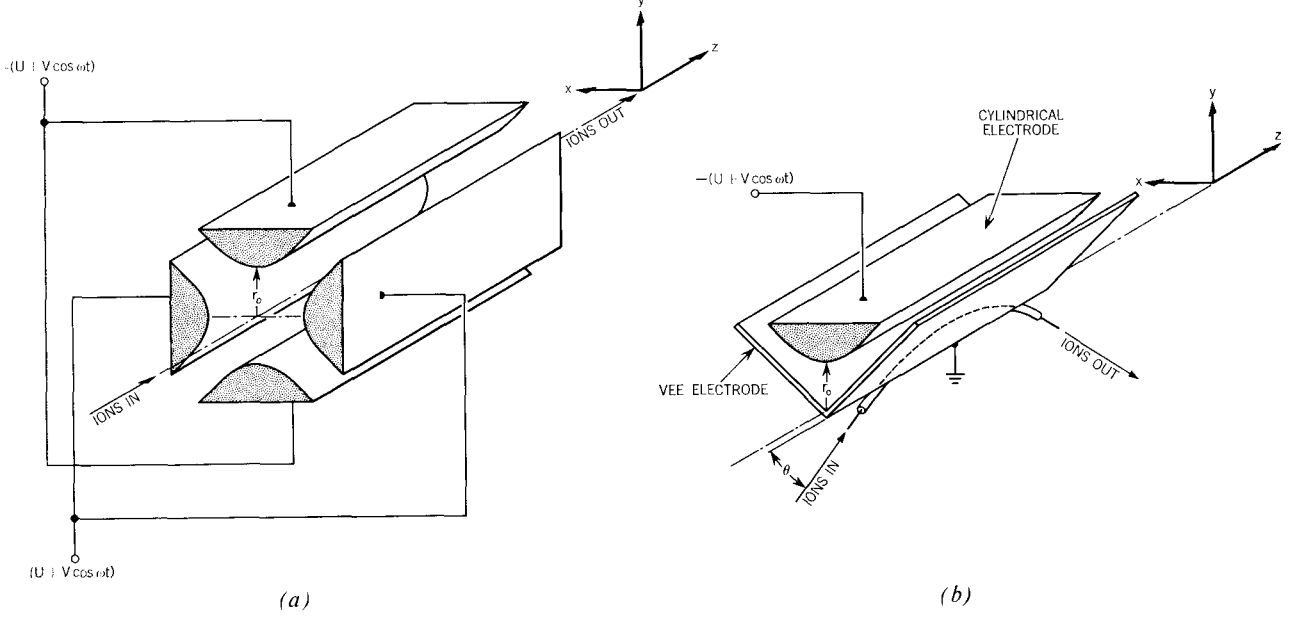


Figure 1 (a) Schematic view of quadrupole mass filter. (b) Schematic view of monopole mass spectrometer with ions injected on the z axis but at an angle to it, with \dot{y} positive. Ions are usually injected parallel to the z axis as described by von Zahn and by Hudson [Refs. 2 and 7].

the injection conditions, i.e., by the accelerating potentials on the ion gun. In the quadrupole mass analyzer, the desired field is achieved by applying potentials of $\pm (U+V\cos\omega t)$ to four electrodes in the configuration shown in Fig. 1(a). In the monopole, Fig. 1(b), the field configuration is achieved by placing a grounded Veeshaped electrode at $y=\pm x,\,y>0$ and an electrode of potential $-(U+V\cos\omega t)$ at $y^2-x^2=r_0^2$. In practice, for reasons of mechanical convenience, the electrodes are in the form of circular cylinders, whose radius R is made equal to 1.15 r_0 in order to minimize the resulting field distortion.^{1,3}

In the monopole instrument the main reason for utilizing only one-quarter of the quadrupole field is to achieve mechanical and electrical simplicity. In the quadrupole, the field pattern has the desired symmetry and shape only if the four electrodes are supplied with voltages of exactly correct amplitude and phase; in the monopole, however, only one electrode must be supplied. In both the quadrupole and monopole instruments it has hitherto been common practice to inject ions close and parallel to the z axis.^{1,2} However, one of the conclusions of this paper is that, for a monopole, the ions should be injected at an angle to the z axis. Figure 1(b) illustrates this recommended mode of operation.

Since the field distribution is identical for both the monopole and quadrupole configurations, the ion trajectories calculated in this paper can be considered to apply to either instrument. However, as is shown in the next section, in the monopole the coincidence of a physical boundary with the ground planes places restrictions on the way in which a monopole can be used and, in practice, the two instruments operate on different principles. In the quadrupole, operating conditions are chosen so that only a narrow band of ion masses describe stable trajectories. Higher masses describe unstable oscillations in the y direction and strike the y electrodes, while lower masses describe unstable oscillations in the x direction and strike the x electrodes. The quadrupole is, therefore, a true mass filter irrespective of the value of v_z , the drift velocity in the z direction. As will be shown, the monopole utilizes ion focussing of the quadrupole field along the z direction and so requires a reasonably well-defined value of v_z . Almost all ions that are eliminated by striking the grounded Vee electrodes are ions that describe stable trajectories and that would be transmitted through a quadrupole instrument.

Mathematical background

The x and y vibrations obey Mathieu's equation 1,2

$$\frac{d^2r}{d\xi^2} + (a + 2q \cos 2\xi)r = 0, (2)$$

where:

$$\xi = \frac{1}{2} \omega t$$
;

for
$$r = x$$
, $a = 8eU/m\omega^2 r_0^2$ and $q = 4eV/m\omega^2 r_0^2$;
for $r = y$, $a = -8eU/m\omega^2 r_0^2$ and $q = -4eV/m\omega^2 r_0^2$.

27

(In Eq. (2), e is the electronic charge and m is the mass of the ion.) If we write M for the mass/charge ratio of the ion in amu /electron, U and V in volts, f the frequency in megacycles \sec^{-1} , and r_0 in centimeters, we have

$$a = 0.196 U/Mf^2r_0^2$$
, $q = 0.098 V/Mf^2r_0^2$

From the above, it is seen that a = 2(U/V)q so that for given U and V the operating point must lie on a straight line through the origin of the (a, q) diagram with slope U/V. The effect of varying ion mass or frequency is merely to shift the operating point along this line.

The drift velocity in the z direction is given by $\frac{1}{2} mv_z^2 = eW \cos^2 \theta$ where W is the ion accelerating voltage and θ the angle of injection relative to the z axis. Hence z is given in terms of ξ by the relation

$$z^{2} = (8eW/m\omega^{2})(\xi - \xi_{0})^{2} \cos^{2} \theta.$$

In the practical units used above, W being in volts, this gives us

$$z^2 = (0.196 W/Mf^2)(\xi - \xi_0)^2 \cos^2 \theta.$$

A mechanical analogy is provided by the motion of the bob of a simple pendulum with mass m and length ldescribing small oscillations under the influence of a periodic force $F\cos \omega t$ vertically downward on the bob. In this case we have $\xi = \frac{1}{2} \omega t$ with $a = 4g/\omega^2 l$, $q = 2F/\omega^2 m l$ for a conventional pendulum (corresponding to the x vibration) and $a = -4g/\omega^2 l$, $q = -2F/\omega^2 m l$ for an inverted pendulum, corresponding to the y vibration. The transformation $\xi = \frac{1}{2} \omega t$ is chosen since, for $q \ll a$, unstable solutions then exist for $a = n^2$ where n is an integer. This reflects the well-known fact that one may "pump up" a garden swing by applying a vertical force at twice the natural frequency of the swing, corresponding to $\omega = 2 (g/l)^{1/2}$, i.e., a = 1. For increasing values of q, unstable solutions to Eq. (2) occur for an increasingly wider range of a values until for values of q comparable to or greater than a, most (a, q) values result in unstable solutions. These results are expressed in the well-known (a, q)diagram. In this paper one is concerned only with the part of the (a, q) diagram rather close to the origin, with q < 0.8 and -0.25 < a < +0.25. The reason for this is that for the monopole one is interested only in stable ion trajectories. For ions to describe stable trajectories in a quadrupole field it is necessary that both the x and y trajectories be stable so that if an (a, q) diagram be superimposed on a (-a, -q) diagram, only those comparatively small areas corresponding to the overlap of stable areas on both diagrams will yield stable ion trajectories. The doubly stable area near the origin is the only one used since the others encompass relatively high values of a and q which are difficult to achieve in practice.

The portion of the (a, q) diagram of interest is shown in Fig. 2. The (a, q) values corresponding to stable solu-

tions lie between the curves a_0 and b_1 representing the stability boundaries. For (a, q) values on a_0 , a solution may be obtained corresponding to the tabulated function $ce_0(\xi, q)$; this function is periodic in ξ with period π and has the interesting property that, for the portion of a_0 shown in Fig. 2, it does not go negative at any value of ξ . The solution so obtained is of little practical use, however, since in general it must be linearly combined with a second solution, which is unstable. Similarly, solutions for (a, q) values on b_1 are, in general, made up of the tabulated function $se_1(\xi, q)$ which is stable with period π , and an unstable solution. However, for (a, q) values lying between a_0 and b_1 a pair of stable solutions $ce_{\beta}(z, q)$ and $se_{\beta}(z, q)$ exist for all (a, q). These have the form a_0

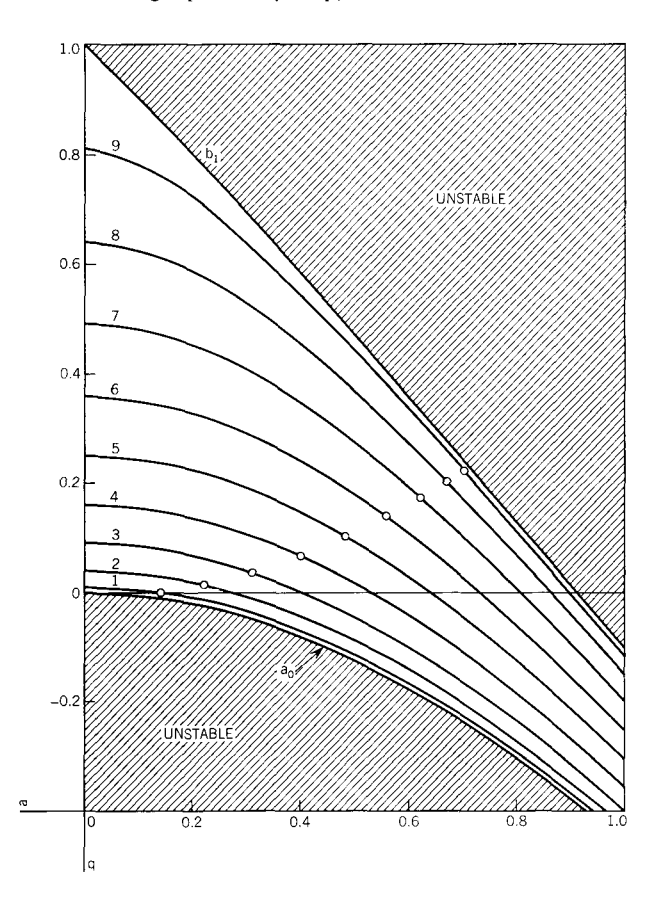
$$ce_{\beta} (\xi, q) = \sum_{n=-\infty}^{\infty} A_{2n}^{(\beta)} (2n + \beta)\xi,$$

$$se_{\beta} (3)$$

where the A_{2n} and β are functions of (a, q) only. In particular, β is a smoothly varying function of (a, q), being 0 on a_0 and 1 on b_1 . In Fig. 1 iso- β lines are plotted for $\beta = p/10$, $0 , in addition to the plots for <math>a_0$ and b_1 .

As pointed out by McLachlan, 4,5 if $\beta = p/s$, where p and s are integers having no common factors, the functions ce_{β} and se_{β} are periodic with a period $2\pi s$ in the variable ξ . However, examination of the form of ce_{β} and se_{β} enables one to go somewhat further than this, depending on whether p is even or odd. Addition of πs to ξ increases all the arguments in Eq. (3) by the quantity $(2\pi ns + \pi p)$. Hence, if p is even, this increase will leave all the terms unchanged, so that ce_{β} and se_{β} will have period πs . On the other hand, if p is odd, all the terms will be increased by an odd number of π 's and, thus, ce_{β} and se_{β} will be inverted. The practical significance of this is as follows: Suppose that both the x and y trajectories could have a period $2\pi s$ in common. In this paper several illustrative families of ion trajectories are shown for which s = 10. This does not imply equal β values, only that β_x and β_y should be rational fractions having s as a common denominator. In this case and for a quadrupole instrument, perfect erect images of the ion source would be formed at intervals of $2s\pi$ in ξ , that is, spatially at z intervals of $4\pi s v_z/\omega$ where v_z is the drift velocity of the ions in the z direction. Unfortunately, this perfect focussing property cannot be utilized in the monopole. While the x vibration is unrestricted except for |x| < y, the y vibration cannot go negative. Since, in describing a complete period all ce_{β} and se_{β} must go negative (with the single exception of ceo which, in practice, is of no value) all the ions would hit the grounded Vee electrode before reaching the first image point. However, if $\beta_y = 1/s$ an inverted y image will

Figure 2 The (a, q) diagram for Mathieu's equation showing the extent of the first stable region and iso- β lines for $0 < \beta < 1$ at β intervals of 0.1. The lines are numbered with the integer p where $\beta = p/10$.



occur at $(\xi - \xi_0) = \pi s$, $(z = sv_z/f)$, where ξ_0 is the value of ξ at z = 0; if the source is a point source on axis, this image will also fall within the instrument, i.e., it will also form on axis. If we also choose $\beta_x = p/s$, $1 \le p < s$, then an x image will likewise occur at the same point, erect if p contains more factors of 2 than s but inverted if not.

The considerations just discussed give the necessary conditions for ions leaving a point source to come to a point focus. That they are also sufficient conditions, in that the y trajectories do not go negative between $\xi - \xi_0 = 0$ and $\xi - \xi_0 = \pi s$ will be demonstrated later by inspection of the trajectories. These restrictive conditions on β_x and β_y mean that the desired double-focusing conditions can be obtained only for certain pairs of (a, q) values; this is illustrated in Fig. 2, where the curves for $\beta = p/10$ are plotted, but where the curves for negative q are not shown since the iso- β curves are symmetrical about the a axis.

From Figure 2 it is seen that if one wishes to work with a y focus at $\xi - \xi_0 = 10\pi$, i.e., $\beta_y = 1/10$, then one must choose (a_y, q_y) values on Curve 1, where $\beta = 1/10$. If an x focus also is desired at the same point, it is necessary that $\beta_x = p/10$. Suppose one decides to make p = 5 so that there will be an x focus at $\xi = 2\pi$, 4π , 6π , 8π , and 10π . One must then choose (a_y, q_y) so that $(-a_y, -q_y)$ will lie on the curve $\beta = 5/10$. Since the iso- β curves are symmetrical about the a axis, this means that $(-a_y, q_y)$ must lie on $\beta = 5/10$. It is possible to choose 9 pairs of (a, q) values in this way corresponding to p = 1, 2, 3, ..., 9. (The value p = 10 giving $\beta_x = 1.0$ is not of practical use since it is on the stability boundary and the x trajectory would be stable only for one particular phase of injection.) These nine points are shown in Fig. 2 and correspond to points where the $\beta = 1/10$ curve, reflected in the q axis, would cut the other iso- β curves. Values of (a, q) for given (p, s) are given in Table 1 (page 30) for 2 < s < 12, 1 . (The method of calculationis described in the appendix).

An example of the use of Table 1 is as follows. Suppose we decide to operate our spectrometer under conditions such that the ions remain in the rf field for exactly 8 rf cycles, i.e., $(\xi - \xi_0) = 8\pi$, or s = 8. This decision restricts our choice of (a, q) values to those lying on the line $\beta_y = 0.125$, which lies just above the line for which p = 1 in Fig. 2. In this way, a y focus is assured. However, we would like also an x focus so that $\beta_x = p/8$, where 0 . Suppose we choose <math>p = 5, then Table 1 tells us that the corresponding (a, q) value is (0.147256, 0.576545).

Calculation of the ion trajectories

Although tabulated values exist for the Mathieu functions of integral order, the calculation of functions of fractional order is not a simple matter. Even after a pair of solutions for a given (a, q) has been found, it would be somewhat tedious to combine them to fit the various initial conditions. Since the ions are injected continually, it is necessary to calculate trajectories for several different phases of injection. It is also necessary to determine the effect of varying the initial values of y and $dy/d\xi$. Even after solutions have been obtained in tabular form, they are very tedious to plot because of their oscillatory nature.

In view of these difficulties, the problem appears to be one that should be solved by recourse to an analog computer, with which it would be possible to obtain output in graphic form, the only input needed being (a, q) and the initial conditions. This could be done, of course, by constructing an inverted pendulum, applying a vertical periodic force of the desired magnitude (by magnetic or other means), and releasing the bob of the pendulum at the desired phase and with the desired initial position and velocity.

[†] The curve b_1 is not symmetrical about the a axis, but its place is taken by curve a_1 , which is obtained by reflection of b_1 in the a axis.

Table 1 Paired values of a [upper] and q [lower] satisfying the condition $\beta(a, q) = 1/s$, $\beta(-a, -q) = p/s$, for 2 < s < 13, $p \le s$. These are operating points for double focusing in the monopole mass spectrometer.

Values of s	Values o	of <i>p</i>	3	4	5	6	7	8	9	10	11	12
3	.000000 .451105	.117076 .656266	.183624 .752057							. , . ,		
4	.000000	.078407 .522848	.166227 .673016	.206116 .732687								
5	.000000 .278436	.053806 .429064	.126186 .575816	.190656 .683276	.216980 .723310							
6	.000000 .233150	.038706 .362294	.095019 .495503	.156067 .610395	. 204406 . 689585	. 223000 . 718107						
7	.000000	.029026 .312945	.073030 .432374	.125161 .542783	.175636 .633358	.212867 .693652	. 226671 . 714933					
8	.000000 .175699	.022510 .275178	.057492 .382516	.100984 .485382	.147256 .576545	.189023 .649155	.218429 .696401	. 229069 . 712857				
9	.000000	.017941 .245420	.046272 .342500	.082550 .437523	.123236 .525286	.163704 .601176	.198534 .660405	.222274	.230721 .711428			
10	.000000 .140869	.014622 .221402	.037966 .309820	.068448 .397543	.103772 .480593	.140909 .555717	.176176 .619571	.205510 .668668	. 225041 . 699745	.231906 .710402		
11	.000000	.012139 .201625	.031673 .282696	.057528 .363872	.088154 .441966	.121500 .514574	.155027 .579307	.185808 .633616	.210768 .674900	. 227097 . 700802	.232785 .709641	
12	.000000 .117532	.010235 .185067	.026802 .259856	.048948 .335236	.075590 .408554	.105293 .477963	.136268 .541700	.166407 .597892	.193377 .644554	.214824 .679707	.228667 .701613	.233455

The procedure actually employed is to use a digital computer to numerically integrate the differential equation, conjoined with an automatic plotter which plots the trajectories from the digital information stored on an output tape. The combination is, in effect, a versatile analog computer, where the differential equation supplies the physical information that is essential for the computer to simulate a pendulum, while the plotting equipment replaces the transducers and display devices that would be required to yield a record of the motion of the bob. This procedure allows one to obtain solutions without any knowledge of the analytic theory of Mathieu's equation.

In the first instance of its use an (a, q) pair was chosen at random somewhere near the stability boundary at a desired (a/q) ratio, and (a, q) values corresponding to a periodic solution were obtained by trial and error. This trial did not, of course, lead to a periodic x trajectory at the same time, and to have attempted to arrive at the (a, q) values for double focusing by trial and error would have been a wasteful procedure. In practice, it has proved more convenient to rely on the analytic theory to provide the (a, q) values needed to obtain solutions of the desired periodicity, as described in the Appendix.

The numerical integration was accomplished by the fourth-order Runge-Kutta method as shown in Fig. 3. The subroutine shown calculates a complete series of y and $dy/d\xi$ values as a function of ξ for given (a, q) and a

specified ξ interval h, which is chosen to be a submultiple of π . The array E is obtained by dividing the number of iterations by the quantity ENQ, and is more convenient than ξ (represented by Z) for reference and plotting purposes. Arrays containing the values of y, $dy/d\xi$, ξ and E are obtained by the instruction

CALL RUNGE (Y, DY, MT, A, Q)

in the main program, the corresponding data for the x trajectory being obtained by

CALL RUNGE (X, DX, MT, AA, QQ)

where MT is the total number of iterations, a=A=-AA and q=Q=-QQ. The arrays are then written on tape for subsequent off-line operation of the plotter. Initial values of ξ , y, $dy/d\xi$, x, $dx/d\xi$ are developed in the main program, the initial value of ξ being transmitted to the subroutine by the "common" statement. Plots of both x and y trajectories were obtained at initial phases ξ_0 of 0, $\pi/16 \cdots 15\pi/16$, and π , and were plotted on the same axes as a function of $\xi - \xi_0$; this procedure provided, in effect, an envelope of spatial trajectories since $z = 2v_z(\xi - \xi_0)/\omega$. Sixteen trajectories were superimposed for all plots shown in this paper. A step size of $h = \pi/50$ was employed for most of the plots.

It was established that the numerical integration was working correctly by applying two criteria:

- (1) Changing the step size h to $\pi/100$ or $\pi/32$ did not materially affect the tabulated output. For $h=\pi/10$ the tabulated output was noticeably different, although this difference would have been barely visible on the plots.
- (2) Perfect focusing was observed at (a, q) values for which the theory predicts perfect focusing.

Results

The types of trajectory obtained when ions are injected on axis, but with finite radial velocity \dot{y}_0 or \dot{x}_0 , are well exemplified in Figs. 4(a) and (b). To aid the eye, curves for trajectories corresponding to $\xi_0=0$ have been made prominent. A whole family of trajectories is shown, corresponding to $\xi_0=0$, $\pi/16$, $\pi/8\cdots 15\pi/16$. The (a,q) value was chosen to give a half period in y of 20π with $\beta_y=1/20$ and $\beta_x=19/20$. It is seen that the image of the source forms on axis, as expected, and, that furthermore, the y trajectories do not go negative at any $(\xi-\xi_0)$ value between 0 and 20π . Hence, if a and q can be maintained constant with sufficient precision, all ions injected at an angle through the point (0,0,0) will pass through

Figure 3 The subroutine used for numerical integration of Mathieu's equation by the fourth-order Runge-Kutta method. The variable ξ is represented by Z.

```
SUBROUTINE RUNGE (V,DV,NT,A,Q)
COMMON H,Z,E,ENQ
DIMENSION E(2500), Z(2500), V(2500), DV(2500)
GRAD(V,Z) = (A+2.0*Q*COS(2.0*Z))*V
DO 20 N=1,NT
A1 = DV(N)*H
B1 = GRAD(V(N), Z(N))*H
A2=(DV(N)+0.5*B1)*H
B2 = GRAD(V(N) + 0.5*A1,Z(N) + 0.5*H)*H
A3 = (DV(N) + 0.5*B2)*H
B3 = GRAD(V(N) + 0.5*A2,Z(N) + 0.5*H)*H
A4=(DV(N)+B3)*H
B4 = GRAD(V(N) + A3,Z(N) + H)*H
V(N+1)=V(N)+(A1+2.0*A2+2.0*A3+A4)/6.0
DV(N+1)=DV(N)+(B1+2.0*B2+2.0*B3+B4)/6.0
EN = N
E(N) = (EN-1.)/ENQ
20 Z(N+1)=Z(1)+EN*H
RETURN
END
```

the point $(0, 0, 20v_z/f)$ without striking the angle electrode in the interval $0 < z < 20v_z/f$. It is of course obvious from the form of the differential equation that if $R(\xi)$ is a solution then $kR(\xi)$ is also a solution where k is a constant. The y and x values in the plots may therefore be scaled in an arbitrary manner. In Figs. 4a, 4b, 5, 6, 7, and 8 the scales on the ordinates are drawn corresponding to initial conditions x_0 or $y_0 = 0$, and $(dx/d\xi)_0$ or $(dy/d\xi)_0 = 1$, but in Figs. 4(c) and (d) the corresponding initial conditions are x_0 or $y_0 = 1$ and $(dx/d\xi)_0$ or $(dy/d\xi)_0 = 0$. The actual initial values fed into the computer were different from unity, and were chosen to give a convenient plot size.

Injection parallel to the axis without radial velocity is shown in Figs. 4(c) and (d). In this case (a, q) is chosen to give $\beta_y = 1/10$, $\beta_x = 1/2$ and a full y period is shown as would exist in a quadrupole instrument. The inverted focussing property for $\xi - \xi_0 = \pi s$, $\beta = p/s$ where p is odd, is well illustrated. Other plots, not shown, were obtained for initial conditions where both y_0 and $(dy/d\xi)_0$ were finite, and similar inverted foci obtained, although generally with somewhat larger amplitudes of oscillation than in Figs. 4(c) and (d). It is seen that about half of the injected ions strike the Vee-electrode after a few rf cycles, as pointed out by von Zahn,2 and although there is a visible tendency for some ions to bunch on the ξ axis just short of $(\xi - \xi_0) = 10\pi$, a good focus is not obtained within the confines of a monopole instrument, i.e., y > 0, |x| < y.

It is clear that injection of the ions on axis but at an angle to it should give superior resolution because of the excellent focussing, and also superior sensitivity, since all the injected ions pass through the instrument, irrespective of their phase of injection. Furthermore, injection through the grounded Vee-electrode could be accomplished with almost no disturbance to the monopole field. Injection parallel to the axis, as presently employed, must inevitably introduce end effects which are almost impossible to calculate and difficult to keep under experimental control.

In Figs. 5 and 6 are shown the x and y trajectories for $\beta_y = 1/10$, $\beta_x = p/10$ where 0 with initial conditions <math>y = 0 or x = 0, and $(dy/d\xi) = 1$ or $(dx/d\xi) = 1$. These plots correspond to operating at (a, q) values coincident with the dots on Fig. 2, and represent all possible trajectories having both x and y foci at $(\xi - \xi_0) = 10\pi$. It is seen that the y vibrations follow a similar pattern irrespective of (a, q) but with a gradually increasing amplitude as we move along the $\beta_y = 0.1$ line to higher q values. The x vibrations are, of course, quite varied in appearance. As will be expected from the considerations in preceding sections, the x vibration has period 20π for p = 1, 3, 7 and 9; 10π for p = 2 and 6; 5π for p = 4 and 8; and 4π for p = 5. Inverted images at the half-period values are formed except for p = 4 and 8. These cor-

respond to β_z values of 2/5 and 4/5 having an even numerator after cancelling, and so the period is 5π , not 10π .

Trajectories obtained for arbitrarily selected β_x and β_y cre essentially similar to those shown in Figs. 5 and 6 axcept that focussing is not usually obtained on the first erossing of the z axis. The effect of varying a and q for a constant a/q is shown in Figs. 7 and 8. In these figures, the portions of the x and y trajectories near $\xi - \xi_0 = 10\pi$ are shown near the operating point $\beta_x = 9/10$, $\beta_y = 1/10$. The (a, q) values are chosen, at intervals of 0.2%, so that a and q take values of from -0.8% to +0.8% greater than the value (0.225041, 0.699745) shown in Table 1. It is seen that an increase of +0.8% results in the y focus being shifted just short of $\xi = 9\pi$. Note that not only do the values of $\xi - \xi_0$ for y = 0 decrease as a and q increase, but also that the focus worsens markedly as one moves away from the value $\xi - \xi_0 = 10\pi$, then improves again as the values 9π and 11π are approached. The operating point chosen is quite near the x stability boundary, and in consequence a considerable increase in the amplitude of the x vibration is observed for a 0.8% increase in a and q.

The remainder of this paper will be mainly concerned with the y trajectory, it being understood that the x trajectories can always be brought to a focus if required by selecting an appropriate β_x . Similar series of curves are obtained for different operating points on the (a, q)diagram. The characteristic movement of the y trajectory envelope, shown in Fig. 7, with good focussing at ξ – $\xi_0 = n\pi$ and only crude focusing effects at $\xi - \xi_0 =$ $(n+1/2)\pi$, is obtained in all cases; the main difference resides in the percentage of variation in q that is required to cause the change. It is of particular interest to relate the variation in z_f , the position of approximate focus, to the variation in q for constant a/q since this gives the spatial mass resolution, mass being inversely proportional to q for given values of the instrument parameters U, V, W and r_0 . However, variation in ion mass changes not only q but also, for a fixed W, the value of v_z ; this change must be allowed for.

As described under "Mathematical background", z is given in terms of $(\xi - \xi_0)$, as

$$z^2 = (8e W/m\omega^2)(\xi - \xi_0)^2 \cos^2 \theta,$$
 (4)

an expression which may be combined with the approximate relation (exact when s is integral),

$$(\xi - \xi_0)_f = \pi/\beta = \pi s,$$

where $(\xi - \xi_0)_f$ is the approximate value of $(\xi - \xi_0)$ for focus. On substituting for $e/m\omega^2$ in terms of q, V and r_0 , one then obtains

$$z_t^2 = 2\pi^2 r_0^2 \cos^2 \theta(W/V) q s^2.$$
 (5)

The spatial mass resolution is then obtained from the variation of qs^2 with q at constant (a/q). This has been

Table 2 Values of q_0 and $qs^2(q-q_0)$ for five different values of a/q. The various s values are tabulated at the right. The table demonstrates that $qs^2(q-q_0)$ is reasonably constant with varying s and is approximately equal to 2.

a/q:	0.	0.066042	.172178	.253562	.321604	Values of
q_0 :	0.	0.132336	.348874	.521757	.673539	S
$qs^2(q-q_0)$	1.904	1.878	1.828	1.778	1.726	4
	1.957	1.938	1.896	1.848	1.795	6
	1.976	1.961	1.922	1.874	1.821	8
	1.984	1.972	1.935	1.887	1.834	10
	1.994	1.985	1.949	1.901	1.848	16
	1.998	1.991	1.957	1.909	1.855	32
	2.000	1.993	1.959	1.911	1.856	64
	2.000	1.994	1.959	1.911	1.857	160

calculated by a method similar to that described in the appendix for obtaining the double focus condition. A binary search on q was made for the condition $a(q, \beta) - (a/q)q = 0$, for given β and (a/q). In this way an approximate empirical relation was found, namely,

$$qs^2 = 2/(q - q_0), (6)$$

where q_0 is the value of q for $\beta=0$ ($s=\infty$) for the (a/q) value in question. Values of the quantity $qs^2(q-q_0)$ are shown in Table 2 for various s values along five different operating lines passing through the points $\beta_v=0.1$, and $\beta_x=0.1$, 0.2, 0.4, 0.6, and 0.9, respectively. The quantity $qs^2(q-q_0)$ is not exactly constant for a given a/q, and its value decreases somewhat with increasing a/q. Nevertheless, the relation is accurate to approximately 10% and, in view of its simplicity, is preferable to the more complex empirical relations which could be devised. The relation is meant to be used only for s>5, i.e., for operating points reasonably close to the line a_0 in Fig. 2. Hence, substituting Eq. (6) in Eq. (5) and differentiating,

$$\Delta z_f/z_f \approx -0.5 \Delta q/(q-q_0) \approx 0.5 \Delta m/(m_0-m),$$
(7)

where m_0 is the mass corresponding to the stability boundary for a given set of operating conditions. Any ion of smaller mass/charge ratio will come to an approximate focus on the z axis within some finite distance from the source. If one substitutes for $(q-q_0)$ in Eq. (7) one obtains what is perhaps the most useful relationship:

$$\Delta z_f/z_f = -(qs/2)^2(\Delta q/q) = +(qs/2)^2\Delta m/m.$$
 (8)

Discussion

The plots shown demonstrate clearly that, for a monopole spectrometer, very exact focusing can be obtained, at

Figure 4 Ion trajectories computed for various initial conditions. The abscissae are $(\xi - \xi_0)$ where ξ_0 is the initial value of ξ . In this and subsequent figures, 17 plots are superimposed corresponding to $\xi_0 = 0$, $\pi/16$, $2\pi/16$, \cdots , $15\pi/16$, π with the plots for $\xi_0 = 0$ and $\xi_0 = \pi$ being identical. For the purpose of visualizing the spatial trajectories, $(\xi - \xi_0)$ may be regarded as equivalent to the spatial coordinate z (Fig. 1). They are related by $z = 2\nu_z^{-1} \omega$ ($\xi - \xi_0$).

Plot $a ext{ ... } y$ trajectory for $y_0 = 0$, $\dot{y}_0 = 1$: a = -.233982; q = -.704396; s = 20; p = 19. Plot $b ext{ ... } x$ trajectory for $x_0 = 0$, $\dot{x}_0 = 1$: a = +.233982; q = +.704396; s = 20; p = 19. Plot $c ext{ ... } y$ trajectory for $y_0 = 1$, $\dot{y}_0 = 0$: a = -.225041; q = -.699745; s = 10; p = 9. Plot $d ext{ ... } x$ trajectory for $x_0 = 1$, $\dot{x}_0 = 0$: a = +.225041; q = +.699745; s = 10; p = 9.

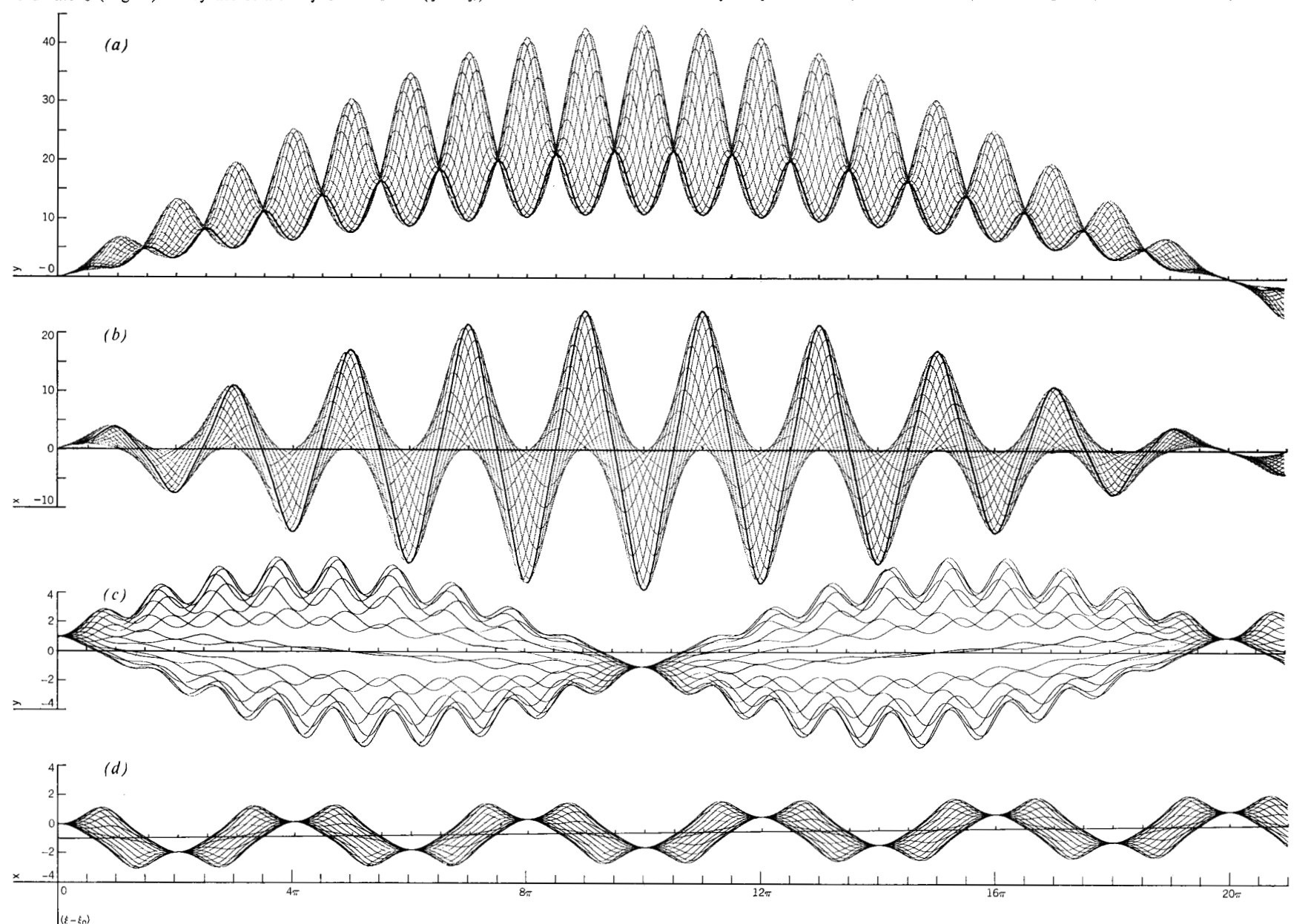


Figure 5 Plots of y trajectories for s=10 and for initial conditions $y=0, \dot{y}=1, 0<\xi_0<\pi$, at intervals of $\pi/16$. Each set of trajectories is for different integral p values 0< p<10 where $\beta=p/10$.

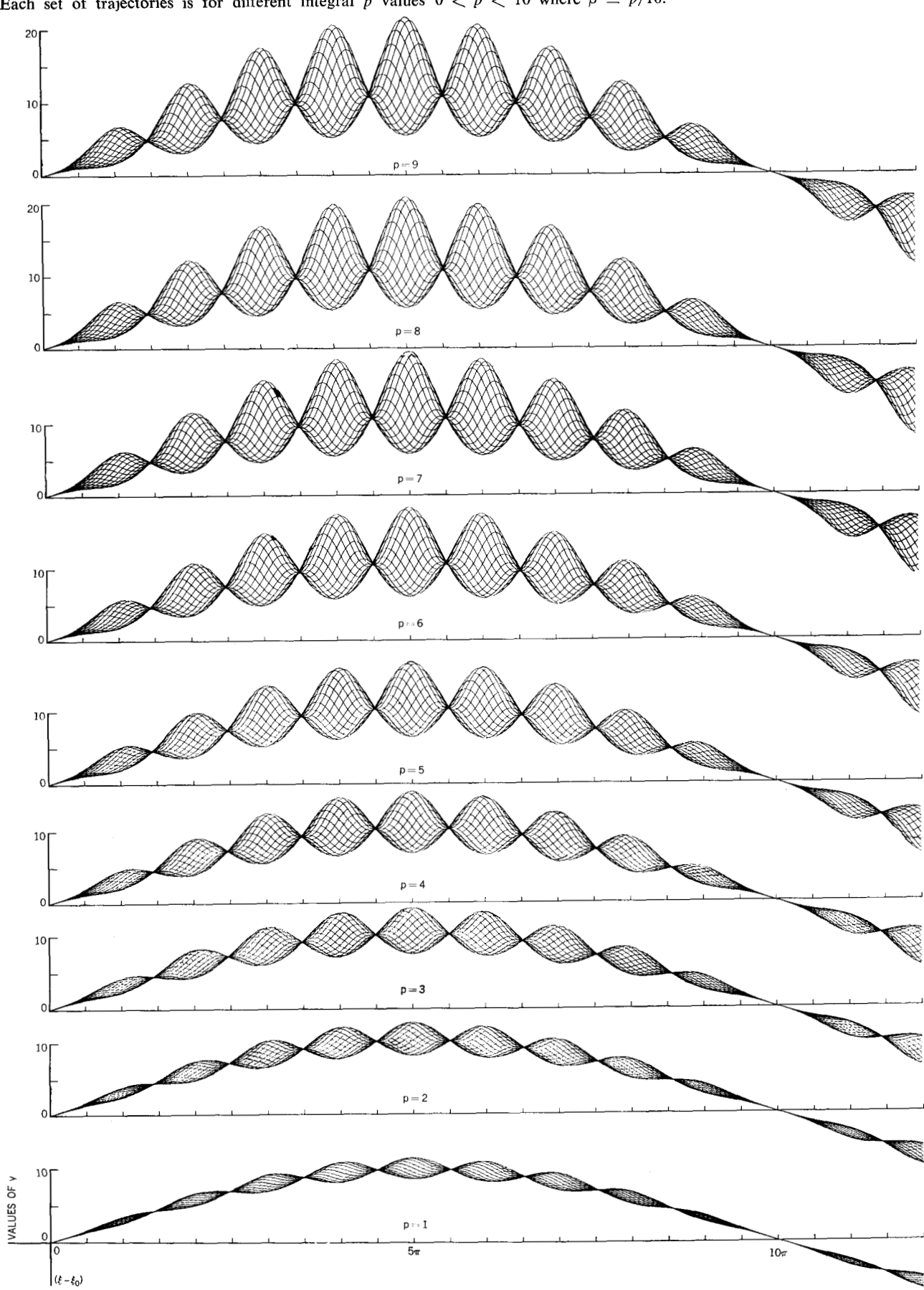
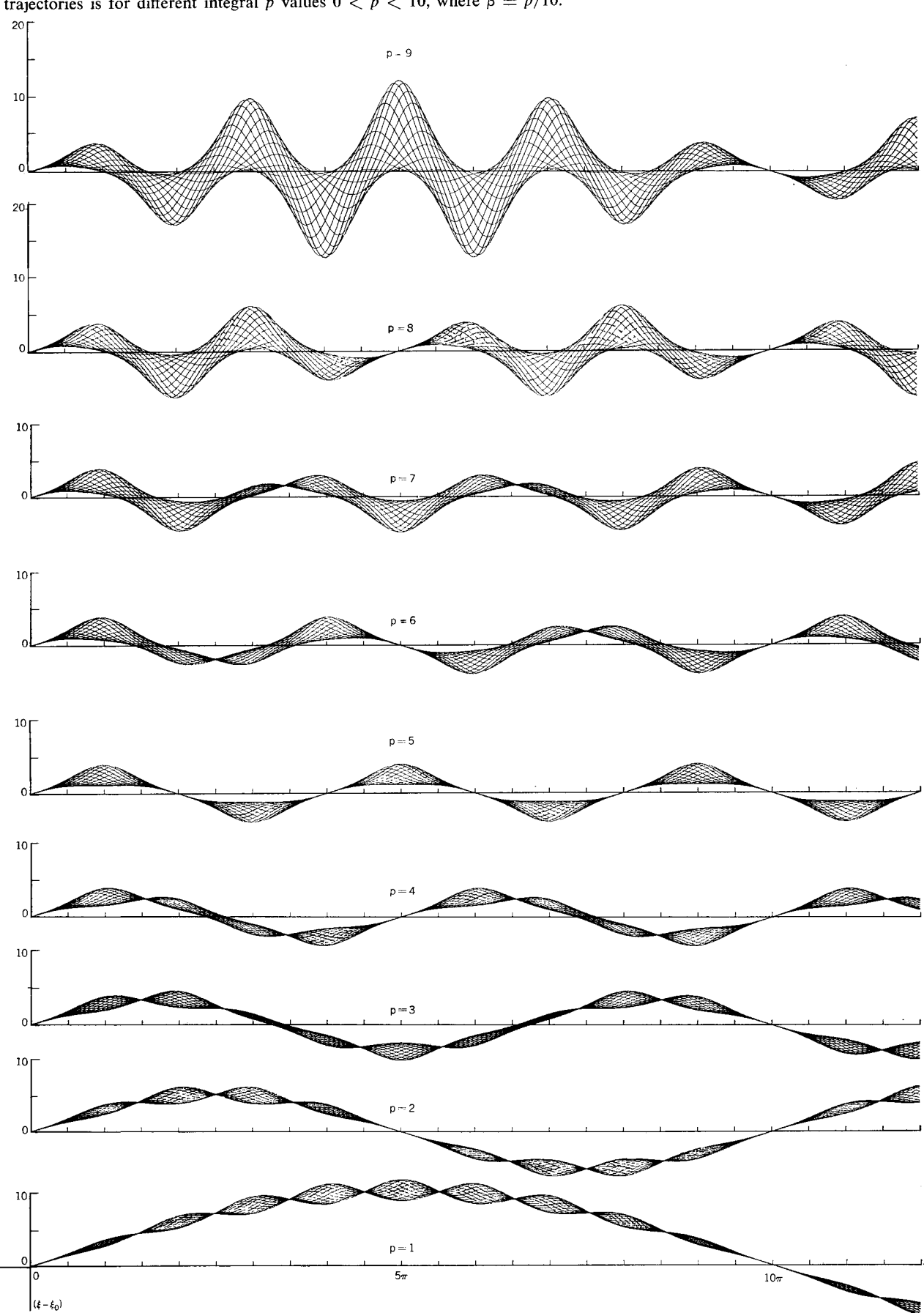


Figure 6 Plots of x trajectories for s=10 and for initial conditions $x=0, \dot{x}=1, 0<\xi_0<\pi$, at intervals of $\pi/16$. Each set of trajectories is for different integral p values 0< p<10, where $\beta=p/10$.



VALUES OF x

least in principle, if the ions emerge from a point source on the z axis. Injection of the ions off the z axis cannot produce a focus within the physical bounds of the instrument, although such a mode of injection is conventional in the quadrupole instrument.2 The trajectories we have shown are applicable to any angle of injection since the x and y vibrations may be multiplied by arbitrary, and different, scaling factors. The angle of injection for the y trajectory should be chosen as large as possible, consistent with the necessity that the desired trajectories not strike the cylindrical electrode at their position of maximum amplitude. This will be satisfied in practice if an undeflected ion beam would strike the cylindrical electrode about three-fourths of the way from the source aperture to the collector aperture. The x trajectories can also be utilized if the ions are deliberately injected with finite \dot{x} , the requirement being that |x| < y for the desired trajectories so that the ions do not strike the Vee electrode.

From Fig. 7 and other plots not presented it is clear that a variation from s = n to $s = n \pm 1$, where n is an integer, results in widely separated trajectory envelopes, each of which cross the axis in a region no greater in extent than the source. It is sometimes convenient to think in terms of the percentage variation in s, regarding s not as an integer but simply as β_y^{-1} . On differentiating the empirical relation of Eq. (6) one obtains

$$ds/s = -[(qs/2)^2 + 0.5] dq/q, (9)$$

and hence, from Eq. (8),

$$dz/z = \left[\frac{q^2s^2}{q^2s^2 + 2}\right] \left[\frac{ds}{s}\right]. \tag{10}$$

Since operating conditions will normally be chosen so that $q^2s^2\gg 2$, one may usually neglect the effect of varying mass on drift velocity and equate dz/z to ds/s. This equivalence is not true, of course, for an operating line a=0 for which $(qs)^2=2$ and dz/z=0.5 ds/s=0.5 dq/q. It is clear that dz/z can never be smaller than this, however, so that even for small values of a/q, when s is chosen large enough an appreciable spatial resolution is obtained. The advantage in working with a nonzero U value is, of course, that qs can be made very large by working close to the stability boundary, s approaching infinity while q remains finite, and very high resolution thereby obtained.

The application of Eq. (9) may be illustrated with reference to Fig. 7, which shows the variation of the trajectories for a $\pm 0.8\%$ variation in q around an operating point for which s=10 and $q\approx 0.7$. This gives $(qs/2)^2=12.25$ and for $\Delta s=\pm 1$, we find $\Delta q/q\approx \mp 0.8\%$ in agreement with Fig. 7. A similar series of figures for s=20 varying about the trajectory shown in Fig. 4(a) gave a variation in s from approximately 19.6 to 20 for $\Delta q/q=0.4\%$. From Eq. (9), with $\Delta s=0.4$, s=20, q=0.7, we obtain

 $(qs/2)^2=50$ and $\Delta s/s=0.02$, hence $\Delta q/q=0.04\%$, which is in agreement with the above. If one supposes that $\Delta s=0.1$ can be resolved, this gives a mass resolution of 0.01% (or 10^{-4}), for s=20, q=0.7. It should be recognized, however, that the excellent focusing characteristic for integral values of s requires not only a perfectly periodic solution, and hence very constant U, V, r_0 , and ω , but also a very low spread in v_z , for otherwise the ions would all cross the z axis at the same time interval after injection, but at slightly different positions.

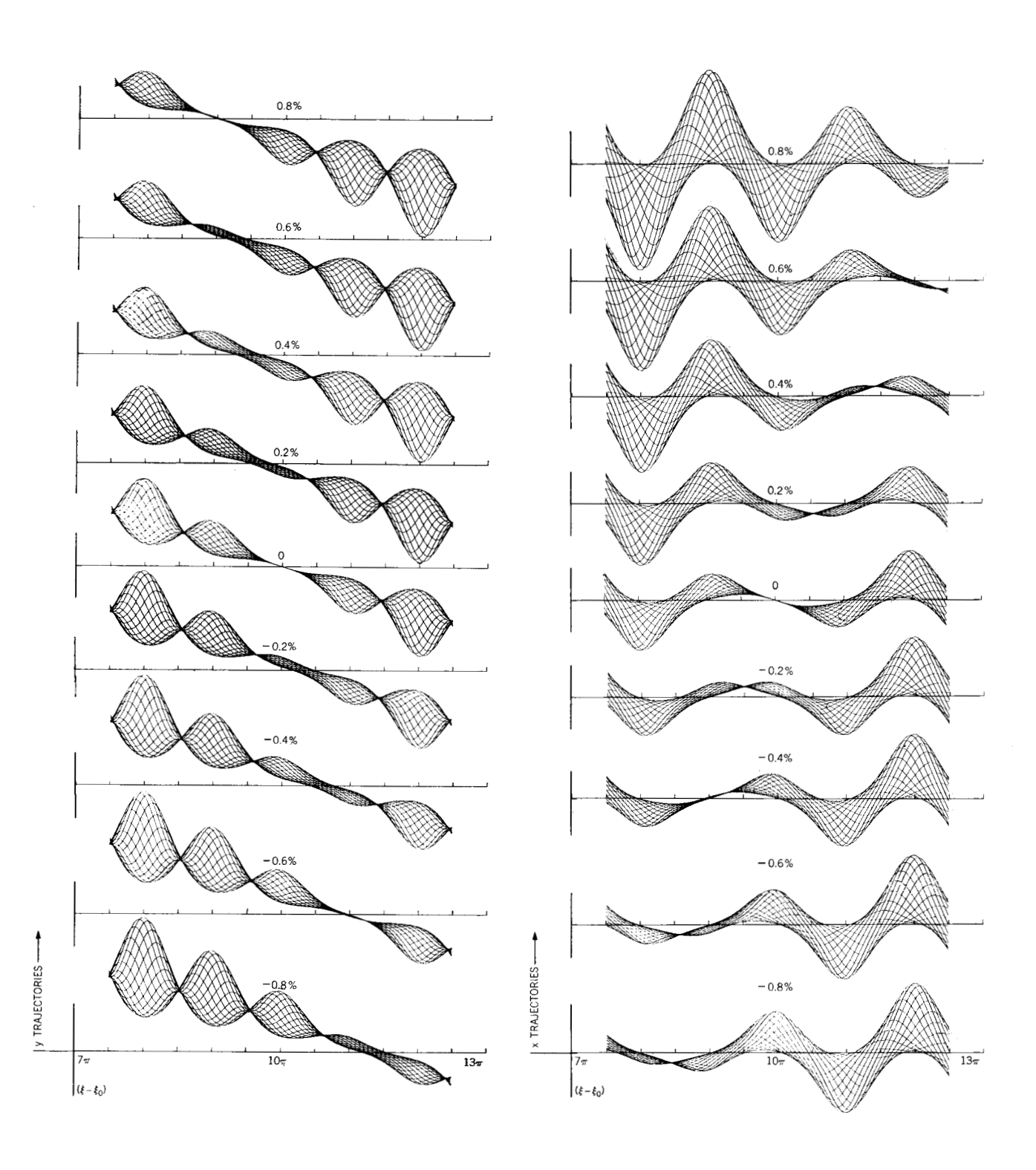
Some typical operating conditions may be derived as follows: Unlike the quadrupole mass filter, the monopole requires reasonably monoenergetic ions since the periodicity in ξ can be translated into a focussing action along the z axis only if v_z is well defined. In order to obtain a reasonably monoenergetic beam of appreciable intensity, an ion accelerating voltage of the order of 100 volts is desirable. Hence, putting $\cos \theta = 1$ and W = 100, one obtains $z^2 = 20(\xi - \xi_0)^2/M_f^2$ from the relation given on page 28. If a convenient length z is taken as 32 cm this gives $(\xi - \xi_0)^2 = 50 \text{ M/}^2$. Writing $\xi - \xi_0 = \pi s$, this gives $s^2 = 5 M f^2$, where M is in atomic mass units per electron and f is in Mc/sec. It is clear that a fairly high frequency is required to enable the ions to experience an appreciable number of cycles of the alternating field within a reasonable length. If one now considers an operating condition for which s = 10, then $f^2 = 20/M$. That is, a range of M from 1 amu/electron to 500 amu/electron would require f to vary from 4.5 Mc/sec down to 200 kc/sec.

One can, of course, scan the mass range by varying U and V keeping U/V constant, provided that W is also varied to ensure that the ions always experience the desired number of rf cycles within the specified length. If this were not done, then the slower, heavier molecules would require a higher value of s to focus in a given length, and the operating point would shift to lower (a, q) values as the mass range was scanned from low to high masses. Since s would not, in general, be integral in such a mode of operation, the good focusing properties associated with integral s values could not be utilized.

Having chosen z, s and W and having obtained the result $Mf^2=20$, we now have $a=10^{-2}U/r_0^2$ and $q=5\times 10^{-3}V/r_0^2$. Hence, if r_0^2 is chosen to be approximately 10 cm² we have $U=10^3a$ and $V=2\times 10^3q$. From Eq. (8) we require qs to be as large as possible for maximum resolution. Let us, therefore, choose $q\approx 0.7$, corresponding to $\beta_x=9/10$, in which case V=1400 volts. Even if we were to choose a=0, giving the minimum value of qs=1.4, we get q=0.14 and V=280 volts. There is, therefore, a requirement for a supply of alternating potential of the order of 1 kV having a precisely defined but variable frequency and an amplitude at least as well defined as the desired mass resolution. Another requirement is that the physical extent of the ion collector

Figure 7 (at left) The effect of varying q at constant a/q on the quality and position of focus for the y trajectory. Initial conditions y=0, $\dot{y}=1$, $0<\xi_0<\pi$, at intervals of $\pi/16$. Each set of trajectories is for different (a,q) values, with (a,q) varying from -0.8% to +0.8% of the operating point (-0.225041, -0.699745) at intervals of 0.2%. Vertical scales are as in Fig. 5.

Figure 8 (at right) As Fig. 7, but for the corresponding x trajectories; i.e., (a, q) = (+0.225041, +0.699745). Vertical scales are as in Figure 6.



must be at least as great as that of the source, together with an allowance for the spread in v_z inevitable in any ion beam. It is of interest to note that if v_z is well defined but has a different value from that for which the instrument has been adjusted, then the mass peaks observed on varying f will be broadened. The system will attempt to produce an "exact" focus after the ions have been in the field for s cycles, s being defined by (a, q), i.e., by U, V, Mf^2 and r_0 . If, however, v_z is too large, this focus will not occur at the collector aperture, but beyond it, and no signal will be detected. In order to bring the ions into the collector it will be necessary to, in effect, reduce s. If frequency scanning is employed this will be done by decreasing the frequency and hence increasing a and q, thereby increasing β_u and hence decreasing s. Since s will thereby have a nonintegral value, the focus will be broadened. If, therefore, the instrument is sufficiently well adjusted that the periodic variation in the quality of focus illustrated in Fig. 7 can be observed as (a, q) is changed at constant a/q, then a variation in W should shift the frequency at which a mass peak is observed and also broaden that peak. This sensitivity of the position of the focal spot to the value of v_z is therefore an advantage, on the whole, since it can be used to provide information on ion energies when the energy is well defined but unknown.

It is instructive to compare the effect of varying ion velocity on apparent mass with the corresponding effect in a magnetic mass analyzer. In the latter case, we have r = mv/eB where r is the radius of curvature of the ion trajectory, B the magnetic induction and v the ion velocity. Clearly, an error in the ion velocity would appear as an equal error in the mass. In the monopole mass spectrometer, an error in v will produce an equal error in z_f , the position of focus. Hence, from Eq. (8) $\Delta v/v = (qs/2)^2 \Delta m/m$.

For large values of qs, a variation in v will have a much smaller effect on the apparent mass than in the case of the magnetic mass analyzer. However, for a=0, then $qs=\sqrt{2}$ and $\Delta v/v=0.5\Delta m/m$ so that if one operates with alternating potential only, the instrument is twice as sensitive to velocity variation as a magnetic mass analyzer. For the operating point shown in Figs. 7 and 8, i.e., $\beta_v=1/10$, $\beta_x=9/10$, qs is equal to 7 and hence $\Delta v/v=12.5$ $\Delta m/m$ so that a 1% change in v will cause only an 0.08% change in apparent mass as observed on the frequency scan. A 1% spread in v would not, therefore, broaden the mass peak very much although it could reduce the sensitivity if the collector aperture were not designed to accommodate such a spread.

Another source of resolution loss is variation in r_0 . Such a variation is mathematically complicated since it transforms the simple Mathieu equation into Hill's equation, for the reason that any spatial variation in r_0 within the range of the instrument, e.g., from $\xi - \xi_0 = 0$ to 10π , can be regarded as a periodic variation in a and q, e.g.,

of period 10π . Furthermore, variations in r_0 necessarily introduce small fields in the z direction and also destroy the complete independence of the x and y vibrations. The latter is also accomplished by the fact that, in practice, the cylindrical electrode is not perfectly hyperbolic and, in fact, is often circular for constructional convenience. However, variations in r_0 have the great advantage of not varying in time. An investigation of the effect of a small variation in r_0 was undertaken by altering the subroutine described by Fig. 3 to allow a variation in a and q from -1% at $\xi - \xi_0 = 0$ to +1% at $\xi - \xi_0 = 10\pi$. When this was done, the trajectories "overshot," crossing the $(\xi - \xi_0)$ axis between $10.3\pi < \xi < 10.6\pi$. Although the average values of a and q were unchanged, this result is not unexpected since the average values of s would be raised, as can be seen from Eq. (6) and Fig. 2. It was found, however, that on increasing a and q at constant a/q until the trajectory envelope straddled $\xi - \xi_0 = 10\pi$, a quite narrow focus was obtained, having a spread in $(\xi - \xi_0)$ of only $\pi/20$. It would, therefore, seem that small variations in r_0 need not be too serious in practice, in that good focussing can be obtained even when Mathieu's equation no longer holds strictly.

Conclusions

- 1) All injected ions of the desired charge/mass ratio can be brought to a focus on the axis of the monopole by correct choice of operating conditions, provided the ions are injected on the axis and at an angle to it. The value of the angle is not critical, but the injection velocity must be well defined.
- 2) Ion trajectories for a given a/q and given initial conditions may readily be generated by numerically integrating Mathieu's equation on a digital computer. These trajectories are readily displayed graphically by plotting off line from an output tape using an automatic plotter.
- 3) Very high resolution can be attained. The main limitation is probably the amplitude stability of the alternating potential.
- 4) Small deviations from perfect geometry do not greatly affect the quality of focus.

Acknowledgments

I am indebted to R. A. Willoughby for indispensable mathematical advice, to F. P. Jona for introducing me to the problem, and to John B. Hudson of the Rensselaer Polytechnic Institute for illuminating discussions. I also thank M. K. Angell and O. Mond for valuable programming advice and assistance.

Appendix: Calculation of (a, q) values for double focussing

Values of a may be calculated for a given q and β by the method described by Tamir. The first step is to calculate three successive iterations of the continued fraction relation

$$a = \beta^{2} - \frac{q^{2}}{(2+\beta)^{2} - a} - \frac{q^{2}}{|(4+\beta)^{2} - a|} - \dots - \frac{q^{2}}{|(2n+\beta)^{2} - a|} - \dots$$

$$- \frac{q^{2}}{(2-\beta)^{2} - a} - \frac{q^{2}}{|(4-\beta)^{2} - a|} - \dots - \frac{q^{2}}{|(2n-\beta)^{2} - a|} - \dots$$

$$(n = 1, 2, 3 \dots).$$
 A-1

Tamir showed that the above iteration converges in an alternating fashion, although sometimes this convergence is very slow; therefore, he tested for "fast" or "slow" convergence and in the latter case took the arithmetic mean of two succeeding iterations as the starting point for the next two.

To avoid this need for a test for convergence rate, the following procedure was adopted. If the first three iterations be denoted by a_{11} , a_{12} and a_{13} then a_{21} , the starting point for the next three iterations, is given by

$$a_{21}-a_{13}=(a_{21}-a_{31})^2/[(a_{21}-a_{31})+(a_{21}-a_{11})].$$

It was found that a_{61} , a_{62} never differed in the seventh place even for $\beta=1$ where the normal iteration procedure was slightly divergent. Five terms were found quite adequate for the summation of each continued fraction. As previously described, the physics of the monopole provides that the a value for the x vibration is minus the a value for the y vibration. If, therefore, we require a pair of

values (a, q) and (-a, -q) such that for the y vibration $\beta_y = 1/s$ and for the x vibration $\beta_x = p/s$, we then require that the quantity $\phi(q) = a(q, \beta_x) + a(q, \beta_y) = 0$, the iso- β lines being symmetrical about the a axis. As can be seen from Fig. 1, $\phi(q)$ is a monotonically decreasing function of q, so that a simple binary search for the condition $\phi(q) = 0$ yields the required q(p, s) and a(p, s). Since the double focusing points for s > 2 occur at q values below 0.8, the search procedure was to start with q > 0.4, $\Delta q = 0.2$, adding or subtracting Δq depending on the sign of ϕ , and halving Δq after each iteration.

The values thus obtained are displayed in Table 1. One cannot, of course, control a and q to six figures in a practical instrument. This degree of accuracy is retained for convenience, in recognition that a six-figure quantity is just as convenient for input to a computer program as a three-figure one; by yielding more exactly the result y = x = 0 at $\xi = s\pi$, the six-figure quantity allows a more sensitive test of the validity of the numerical integration.

Nomenclature

- a Coefficient occurring in Mathieu's equation. In the monopole mass spectrometer, $a = 0.196 \text{ V/Mf}^2 r_0^2$.
- a_0 , b_1 Curves denoting stability boundaries on the (a, q) diagram, as in Fig. 2
- e Electronic charge
- f Frequency of alternating potential in Mc/sec
- m Mass of ion
- M Mass/charge ratio of an ion, in amu/electron
- p Integer used in specifying operating point
- q Coefficient occurring in Mathieu's equation. In the monopole mass spectrometer $q = 0.098 \text{ V}/M_1^2 r_0^2$.
- r_0 The closest distance between the cylindrical electrode surface and the z axis (Fig. 1)
- s Equal to $1/\beta_{\nu}$. In this paper, s is usually an integer except in the discussion section.
- U Steady potential applied to the cylindrical electrode

- v_z Drift velocity along the z direction.
- V Alternating potential applied to the cylindrical electrode
- W Energy, in eV, with which ions enter the instrument x, y, z Spatial coordinates as in Fig. 1
- Z Used for ξ in Fig. 3
- β Quantity occurring in the solution of Mathieu's equation [See Eq. (3)]. In general, if $1/\beta$ is an integer, the corresponding solutions of Mathieu's equation will have period $2\pi/\beta$ in ξ .
- β_x Value of β for the x trajectory, usually equal to p/s.
- β_y Value of β for the y trajectory. It is equal to 1/s.
- Dependent variable in Mathieu's equation, equal to $\frac{1}{2}ωt$
- θ Angle which injected ions make with the z axis
- ω Angular frequency of the alternating potential in radians \sec^{-1}

References

- W. Paul, H. P. Reinhard, and U. von Zahn, Z. Physik 152, 143 (1958).
- 2. U. von Zahn, Rev. Sci. Inst. 34, 1 (1963).
- I. E. Dayton, F. C. Schoemaker, and R. F. Mozley, Rev. Sci. Inst. 25, 485 (1954).
- 4. N. W. McLachlan, Phil. Mag. 36, 403 (1945).
- 5. N. W. McLachlan, *Theory and Application of Mathieu Functions*, Oxford University Press, 1951, pages 79-81.
- This was also pointed out by von Zahn. See page 2 of Ref. 2.
- John B. Hudson, American Vacuum Society—11th National Symposium, 1964 (unpublished).
- 8. T. Tamir, Math. Comp. 16, 77 (1962).
- Calculations were programmed in FORTRAN IV, run on an IBM 7094 computer, and plotted output obtained on an IBM 1627 plotter.

Received August 5, 1965.